Recent Advances on III-Nitride Nanowire Light Emitters on Foreign Substrates – Toward Flexible Photonics

Haiding Sun and Xiaohang Li**

Flexible electronic and photonic devices have received broad interest in the past, due to their compact size, new functionalities, and other merits which devices on rigid substrates do not possess. In this context, the author review recent progresses on flexible III-nitride nanowire photonic devices, focusing on LEDs and lasers. The formation of III-nitride nanowire LEDs and lasers directly on various foreign substrates is firstly described, paving the way to flexible III-nitride nanowire photonic devices through either direct growth on or transfer to flexible substrates. The realization of flexible III-nitride nanowire LEDs through various transfer processes is further detailed. In the end, the challenges of III-nitride nanowire technology for flexible integrated photonics are discussed.

1. Introduction

III-nitrides (InN, GaN, AlN) and their alloys have a tunable energy bandgap from the near-infrared (InN, 0.65 eV) to the deep ultraviolet (AlN, 6.1 eV) by changing the alloy composition. This tunable and direct bandgap enables III-nitrides to be exploited in optoelectronic/photonic devices, including light emitting diodes (LEDs), lasers, detectors, and solar cells.[1,2] Though the success of GaN epilayer technologies in blue/blue–green spectral range, their extension to ultraviolet (UV) and near-infrared (NIR) has been lagging behind, by and large, due to the high defect/dislocation densities and poor p-type doping as more In and Al are incorporated.[3] Moreover, these photonic devices are mostly built on sapphire, bulk GaN, and SiC substrates,[4–10] which are rigid, and cannot meet the growing demand for new functionalities, for example, wearable devices, which require flexible electronic and photonic device components. Although using mechanical polishing,[11] mechanical peeling off,[12,13] dry techniques such as laser lift-off,[14–18] and epitaxial lift-off such as selective wet etching of sacrificial layer[19–21] or entire substrate,[22] these rigid substrates can be removed and III-nitride epilayers can be transferred to flexible substrates. These substrate removing processes, together with the subsequent processing steps to fabricate and assemble the micro- and nano-scale devices for flexible photonics, are highly complicated; and how to maintain the quality of the epilayers at a large scale has remained challenging.[23,24]

On the other hand, driven by the chip size scale-down and the ability to integrate electronic and photonic components on a single chip, GaN nanowire based photonic devices are investigated.[25,26] Not only sparkled by the new integration technology but more fundamentally, GaN nanowires, compared to GaN epilayers, have a number of fundamental advantages from the materials point of view, which could overcome the challenges confronting GaN epilayer technologies and deliver devices that were otherwise unattainable. These fundamental advantages, to a large extent, originate from the large surface to bulk volume ratio: 1) As the nanowire lateral dimension reduces, the critical thickness approaches infinity, which indicates a much-improved material quality, for example, reduced stacking faults and threading dislocation densities.[27,28] 2) Due to the reduced lattice strain imposed by surface dopants compared to bulk dopants, doping, especially p-type doping, can be much more efficient, compared to epilayers.[29–36] For example, recent studies have demonstrated the unmatchable electrical performance of AlN nanowire LEDs,[36] comparing to c-plane AlN LEDs. The very efficient p-type doping also enables electrically injected semiconductor lasers in the deep UV band.[37–39]

On top of these fundamental advantages from the materials aspect, III-nitride nanowires can be formed virtually on any foreign substrates. This immediately enables their unrivaled capability in integration, not only with the existing Si CMOS technology for Si photonics,[40] but also with other devices and systems for flexible integrated photonics. In the past decade, much exciting progress has been achieved in the development of III-nitride nanowire heterostructures on various foreign substrates, including Si, metal, diamond, and two-dimensional (2D) materials.[39,41–45] Various nanowire transfer techniques have also been demonstrated, which represents a viable path toward III-nitride nanowire based flexible integrated photonics.[25,46,47]

These growth for III-nitride nanowires can be found in recent review articles.[2,48,49] In this paper, we focus on photonic devices, in particular LEDs and lasers. In Section 2, we describe III-nitride nanowire LEDs and lasers on various foreign substrates, including Si, metal, diamond, and 2D materials, for example, transition metal dichalcogenides (TMDCs), manifesting the capability of forming III-nitride nanowire device structures on various

Dr. H. Sun,[+] Dr. X. Li
King Abdullah University of Science and Technology (KAUST)
Advanced Semiconductor Laboratory
Thuwal 23955, Saudi Arabia
E-mail: haiding@ustc.edu.cn; xiaohang.li@kaust.edu.sa

[+]Current address: School of Microelectronics, University of Science and Technology of China, Hefei, Anhui 230026, China.

The ORCID identification number(s) for the author(s) of this article can be found under https://doi.org/10.1002/pssa.201800420.

DOI: 10.1002/pssa.201800420

substrates, which provides an elegant path to realize flexible III-nitride nanowire photonic devices through either direct growth or transfer. In Section 3, we discuss flexible III-nitride nanowire LEDs through various transfer processes. Conclusions and prospects of III-nitride nanowires for flexible integrated photonics are made in Section 4.

2. III-Nitride Nanowire Photonic Devices Fabricated Directly on Foreign Substrates

Different from the growth of III-nitride epilayers, wherein the epitaxial relationship (lattice matching) with the substrate is required, recent studies have suggested that the growth of III-nitride nanowires can take place essentially on any substrates. Some of the examples include: InN nanowires grown on bare glass substrates,[50] GaN nanowires grown on amorphous Al_xO_y,[51] GaN nanocolumns grown on silica and quartz,[52,53] AlN nanowires synthesized on carbon nanotubes,[54] and GaN nanowires grown on sapphire.[55] Moreover, further beyond these growth efforts, III-nitride nanowire LEDs and lasers on Si, metal, diamond, and 2D materials have also been demonstrated.[36,37,41–47,56–59] In what follows, we describe these progresses.

2.1. Growth Tactics of III-Nitride Nanowire

The growth/synthesis of III-nitride nanowires has been developed for decades, pioneered, among others, by Lieber et al.,[60] Calleja et al.,[61] and Kishino et al.[62] Different synthesis techniques, including chemical vapor deposition (CVD),[63,64] metal-organic chemical vapor deposition (MOCVD),[46,65] and molecular beam epitaxy (MBE)[66–68] are widely adopted to fabricate III-nitride nanowires. In particular, tremendous effort was devoted to controlling nanowires' density, doping, and morphology.[2] While these growth techniques vary from each other, the underlying mechanisms mainly fall in two categories: the vapor–liquid–solid (VLS) and the diffusion-driven growth process. Both CVD and MOCVD fall in the category of VLS process, involving adatom adsorption, diffusion, and precipitation.[69] Such VLS-driven growth, in most cases, naturally relies on foreign metal catalysts (namely "seeds") to initiate the nucleation process.[70] But, the additional step of seed deposition complicates the fabrication process, and the seeds may further introduce unintentional doping or create unexpected defects in nanowires which affect optical and electrical properties.[71] Therefore, the diffusion-driven mechanism, a completely catalyst-free process, becomes more popular. MBE is a typical tool operating under this mechanism, and the growth is a combination of thermodynamical and kinetical process,[61,62,67,68,71] normally following two-step: a self-nucleation process driven by the atom diffusion and subsequent steady 3D anisotropic growth. The impinging flux and growth temperature are major parameters which govern the initial nucleation process and affect the lateral and vertical growth of nanowires subsequently.[62] A full understanding of these specific growth condition is the prerequisite for achieving high quality nanowires. Nowadays, the MBE process can be carefully monitored from the nucleation to steady growth via in-suit reflection high-energy electron diffraction (RHEED).[67,68]

Haiding Sun received his PhD (2015) in Electrical Engineering from Boston University. His research interests include the investigation of the physics, MBE and MOCVD epitaxy, fabrication, and characterization of semiconductor materials and devices. This includes nanostructures and low-dimensional structures (quantum wires, dots, wells) for nanoelectronics and nanophotonics, based on group III-Nitrides.

Xiaohang Li is an Assistant Professor of Electrical Engineering and the PI of the Advanced Semiconductor Laboratory at KAUST. His research focuses on optical and electronic devices, physics, and equipment based on wide-bandgap semiconductors. He received Ph.D. in Electrical Engineering from Georgia Institute of Technology.

More recently, the selective area growth (SAG) of III-nitride nanowires by pre-patterning the substrate has been increasingly popular to overcome the challenges associated with the randomness of nucleation process in the spontaneous formation of those nanowires. Morphologically homogeneous and highly ordered III-nitride nanowire arrays can be realized by designing the mask layer including the opening size and pitch.[66,72] The SAG process can be realized by both MBE[68] and MOCVD[72] technique, and the nanowires start with nucleation via adatom diffusion on the opening area of the patterned substrate and subsequently grow upward with stable hexagonal shape. With this approach, extra patterning process to define the mask by e-beam lithography technique or nano-imprint technique, if the patterning process covers a large area, is quite time consuming and cost ineffective. Thus, the III-nitride nanowires produced by spontaneous formation is still the mainstream approach. Particularly, the nanowire growth on various substrates is a subject worthy of further investigation, which is also critical to improve the device performances on these unconventional substrates. For more detailed growth control over the density, doping, morphology and material quality of such nanowires, readers may refer to the earlier review and book chapters.[2,48,49,73]

2.2. III-Nitride Nanowire LEDs and Lasers on Si Substrate

Si has been the backbone of modern information technology. From the integrated Si-photonics point of view, and moreover, the low cost of Si substrate, it is natural to explore III-nitride nanowire photonic devices on Si substrate.[2] Furthermore, Si substrate can be easily removed, making it suitable for various transfer processes and enabling device transfer to flexible substrates (we will give such samples in Section 3).[47]

In the past decade, III-nitride nanowire light emitting devices on Si substrate have been explored intensively, covering from deep UV to visible spectral range.[2] In the visible spectral range, InGaN-based nanocolumn LEDs[66,67] and InGaN/GaN dot/disk-in-nanowire LEDs with emission wavelengths in red/green/blue (RGB), with output power up to 30 mW, have been demonstrated.[74,75] Furthermore, using similar InGaN nanowire structures, green and red edge emitting lasers have been reported.[76,77] Moreover, with the use of SiO_x patterning on Si substrate, RGB emission has been exemplified on a single Si chip.[78] Aside from using InGaN as active region, AlInGaN quaternary nanowire LEDs with emission wavelengths widely tunable from blue to red have been demonstrated.[79] Recently, with using selective area epitaxy on SiO_x patterned Si substrate, flicker-free InGaN nanowire LEDs operating at 60 Hz have also been demonstrated.[80]

In the ultraviolet spectral range, the development of Al-rich AlGaN nanowires for achieving unprecedented deep UV photonics is embraced by the nitride community.[36,37] Due to the fundamental advantages of low defect/dislocation densities and efficient p-type doing, AlN nanowire deep UV LEDs emitting around 207 nm (room temperature) with unmatchable electrical performance, comparing to c-plane AlN LEDs, have been demonstrated.[36] The very efficient p-type doping also enables electrically injected semiconductor lasers in the deep UV band using AlGaN nanowires.[37–39] In what follows, we describe these two important progresses in the deep UV photonics with Al(Ga)N nanowires on Si, as examples.

2.2.1. AlN Nanowire Based LEDs

Such short wavelength LEDs are formed by pure AlN nanowires, which are self-organized on Si substrates by MBE.[36,81] The device is in the form of AlN p-i-n junction. A schematic of AlN nanowire LEDs is shown in **Figure 1**(a). The current–voltage (I–V) characteristics measured at room temperature are shown in Figure 1(b). It is seen that, compared with the extreme high turn-on voltage of 20–40 V measured from the conventional c-plane AlN LEDs,[82] the AlN nanowire LEDs have a turn-on voltage of only around 5.5 V. This significantly improved electrical performance is largely attributed to the enhanced Mg dopant incorporation in AlN nanowires, and the minimized unwanted contamination with the use of ultrahigh purity source materials and ultrahigh vacuum in the MBE environment. Furthermore, the use of nitrogen rich environment during the MBE growth that can minimize the nitrogen vacancies (defect donors).[36] The Electroluminescence (EL) spectra under different injection currents are shown in Figure 1(c). It is seen that strong emission is measured at 207 nm.[36] Recently, AlN/BN nanowire LEDs have also been demonstrated.[83] Different from AlN nanowire p-i-n LEDs, such AlN/BN nanowire LEDs do not have any intentional p-type doping. Instead, p-type background doping of h-BN is utilized. With such AlN/BN nanowire structures, the light emission is improved by more than one order of magnitude, as shown in Figure 1(d). This light improvement is attributed to more efficient hole injection and carrier confinement in the active region with the use of h-BN.[83] Both diodes have similar turn-on voltages (5.5 V) and EL spectra with single peak emission, except a 3 nm blue shift for the AlN based p-i-n diode.

2.2.2. Electrically Pumped AlGaN Ternary Nanowire Deep UV Lasers

Electrically injected deep UV lasers have recently been achieved with the MBE grown Al-rich AlGaN nanowires on Si.[37–39] Such deep UV lasers are based on the light Anderson localization effect, as schematically shown in **Figure 2**(a). Detailed simulations indicate that Q factor up to 10 000 can be realized.[84] On the other hand, the vertical optical field is confined through the tapered nanowire morphology – an index guiding through effective index variation. The device fabrication follows standard photolithography and metallization processes.[37] The EL emission spectra under different injection currents for a device emitting at 239 nm is shown in Figure 2(b). It is seen that at a low injection current, only a broad emission is measured; and as more currents are injected, a sharp peak around 239 nm is measured. The light–current (L–I) curve is shown in Figure 2(c),

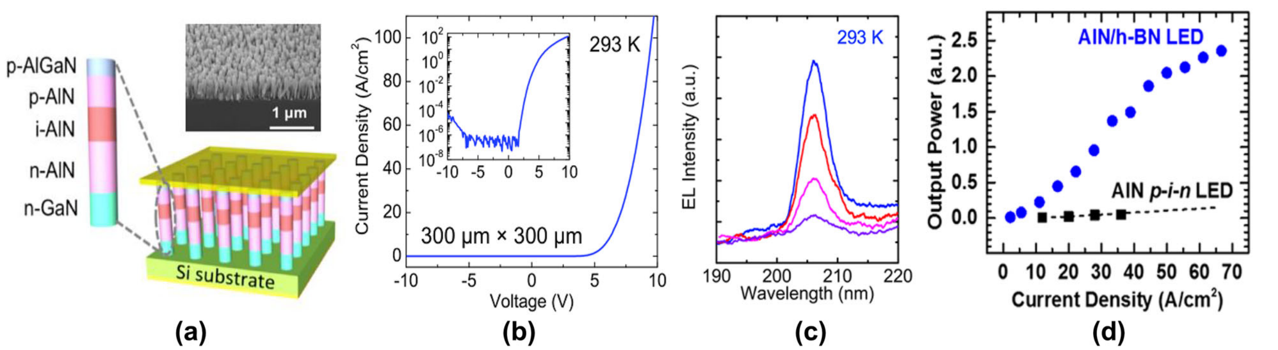

Figure 1. a) Schematic of AlN nanowire LEDs. The inset shows an SEM image of AlN nanowires. b) I–V characteristics measured at room temperature, with the inset showing the characteristics in a semi-log scale. c) EL spectra measured from AlN nanowire LEDs under different injection currents (28–110 A cm^{-2}, pulsed). d) A comparison of light intensity between AlN nanowire p-i-n LEDs and AlN/BN nanowire LEDs. a) Reproduced with permission.[36] Copyright 2015, Macmillan Publishers Limited. b,c) Reproduced with permission.[81] Copyright 2015, American Chemical Society. d) Reproduced with permission.[83] Copyright 2017, American Chemical Society.

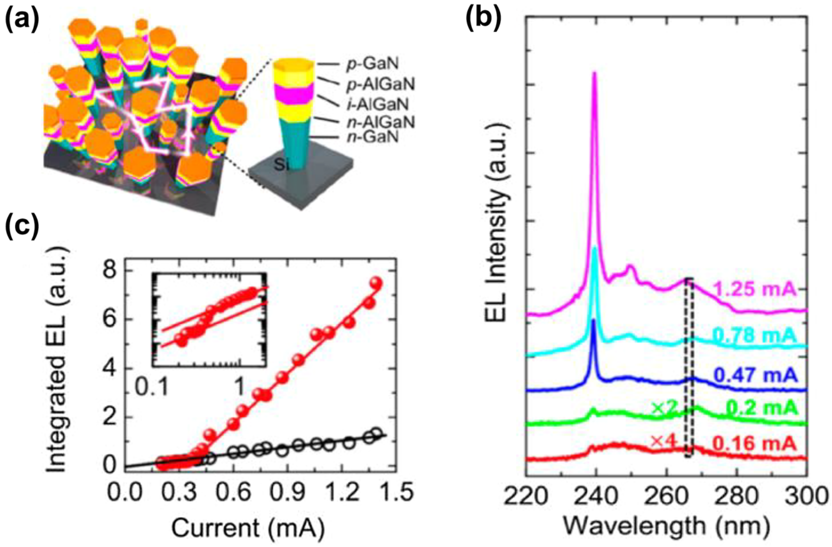

Figure 2. a) Schematic of the cavity formation and each layer of an individual AlGaN nanowire. b) Lasing spectra under different injection currents. c) L–I curve of the lasing peak (red filled circles) and non-lasing cavity mode (black open circles) taken from the boxed region in (b). The inset shows the lasing peak in a logarithmic scale. Reproduced with permission.[37] Copyright 2016, the AIP Publishing.

exhibiting a threshold around 0.35 mA. The logarithmic scale plot of L–I curve shows the transition from spontaneous emission, amplified spontaneous emission, to lasing (inset of Figure 2[c). The non-lasing cavity mode is also examined. As shown by black open circles, the intensity only exhibits a small increase above the threshold. By further changing the cavity design and alloy composition, such electrically injected AlGaN nanowire lasers can operate in nearly entire UV spectral range. This realization of electrically injected lasing in the entire UV band is ascribed to the use of nearly defect-free AlGaN nanowires, the drastically improved hole concentration, the presence of high Al content AlGaN shell that reduces surface nonradiative recombination process, and the excellent optical confinement due to the strong light localization in randomly arranged AlGaN nanowires.[37–39,84]

2.3. III-Nitride Nanowire LEDs on Metal

Though progresses of III-nitride nanowire LEDs and lasers on Si substrate, the formation of the insulating amorphous Si_xN_y layer[85] as the active nitrogen radicals impinge upon the Si surface hinders vertical carrier transport and heat dissipation near the nanowire/Si interface. Furthermore, significant UV and deep visible light absorption by Si substrate reduces light extraction efficiency. Removing Si substrate, or using reflective interfacial metal layers could be necessary to improve the device performance. Additionally, a substrate that has a better thermal conductivity than Si is preferred for high power operation. In this regard, utilizing low cost metal substrates could be a promising solution.

GaN nanowires grown on metals, such as metallic titanium nitride (TiN) film and titanium (Ti) foil, have been reported recently.[86–88] Moreover, GaN nanowire based LEDs fabricated on metals emitting in the UV and visible spectral range have also been demonstrated, including blue to green LEDs on molybdenum (Mo)-coated Si substrate;[41] orange LEDs on Ti-coated Si substrate;[57] red LEDs on Ti-coated Mo substrate[45] and yellow LEDs on Ti-coated Si substrate;[89] UV LEDs (310–380 nm) on tantalum (Ta) foil,[58] Ti-,[90] and tantalum nitride (TaN)-[91] coated Si substrate. In this section, we discuss III-nitride nanowire LEDs on metal substrates and/or metal-coated Si substrates.

2.3.1. III-Nitride Nanowire LEDs on Ti-Coated Si Substrate

InGaN nanowire true yellow LEDs[89] and AlGaN nanowire UV LEDs on Ti-coated Si[90] have been recently developed. **Figure 3**(a) shows the high angle annular dark field scanning transmission electron microscopy (HAADF-STEM) image of vertically aligned AlGaN nanowires grown on Ti-coated Si substrate. Figure 3(b) presents the light output power–current–voltage (L–I–V) characteristics of a 337 nm emitting UV LED fabricated on such a substrate, with a mesa size of 500 μm × 500 μm. The device has a turn-on voltage of about 5.5 V, and the light intensity increases almost linearly as the injection current increases. The device performance is further improved after treating with diluted potassium hydroxide (KOH) solution.[92] Shown in Figure 3(c,d), about 50% enhancement of output power, together with improved I–V characteristics, has been measured. This enhancement is attributed to the removal of the surface dangling bonds and oxidized nitrides (Ga—O or Al—O bonds) at the surface, and the success in mitigating Shockley–Read–Hall recombination. A similar passivation study has also been performed for InGaN/GaN nanowires.[93]

2.3.2. III-Nitride Nanowire LEDs on Ti-Coated Mo Substrate

Zhao et al. further reported red color emitting (≈710 nm) In rich InGaN/GaN quantum-disk-in-nanowire LEDs on Ti-coated Mo substrate.[45] **Figure 4**(a) shows a schematic of the fabricated device. The inset shows the HAADF-STEM image of an individual InGaN/GaN nanowire. The EL spectra under different injection currents are shown in Figure 4(b). Figure 4(c) shows the L–I–V characteristics of an LED with a mesa diameter of 400 μm measured under dc injection. The inset shows the charge-coupled device (CCD) image for a uniformly illuminated LED. A low turn-on voltage of around 2 V is due to the absence of interface amorphous layer (Si_xN_y), which is often observed in nanowires grown on Si.[85] At an injection current of 500 mA, the output power is 6.14 mW, which is considerably higher than the previously reported InGaN/GaN quantum well LEDs emitting at a similar wavelength.[94] Furthermore, a device lifetime test shows a stable operation up to 8 h,[45] far beyond the lifetime of similar devices on Si.[85] Detailed studies further suggest that metal substrates not only offer an efficient heat dissipation channel, but also act as an effective n-type contact as well as an optical mirror.[95]

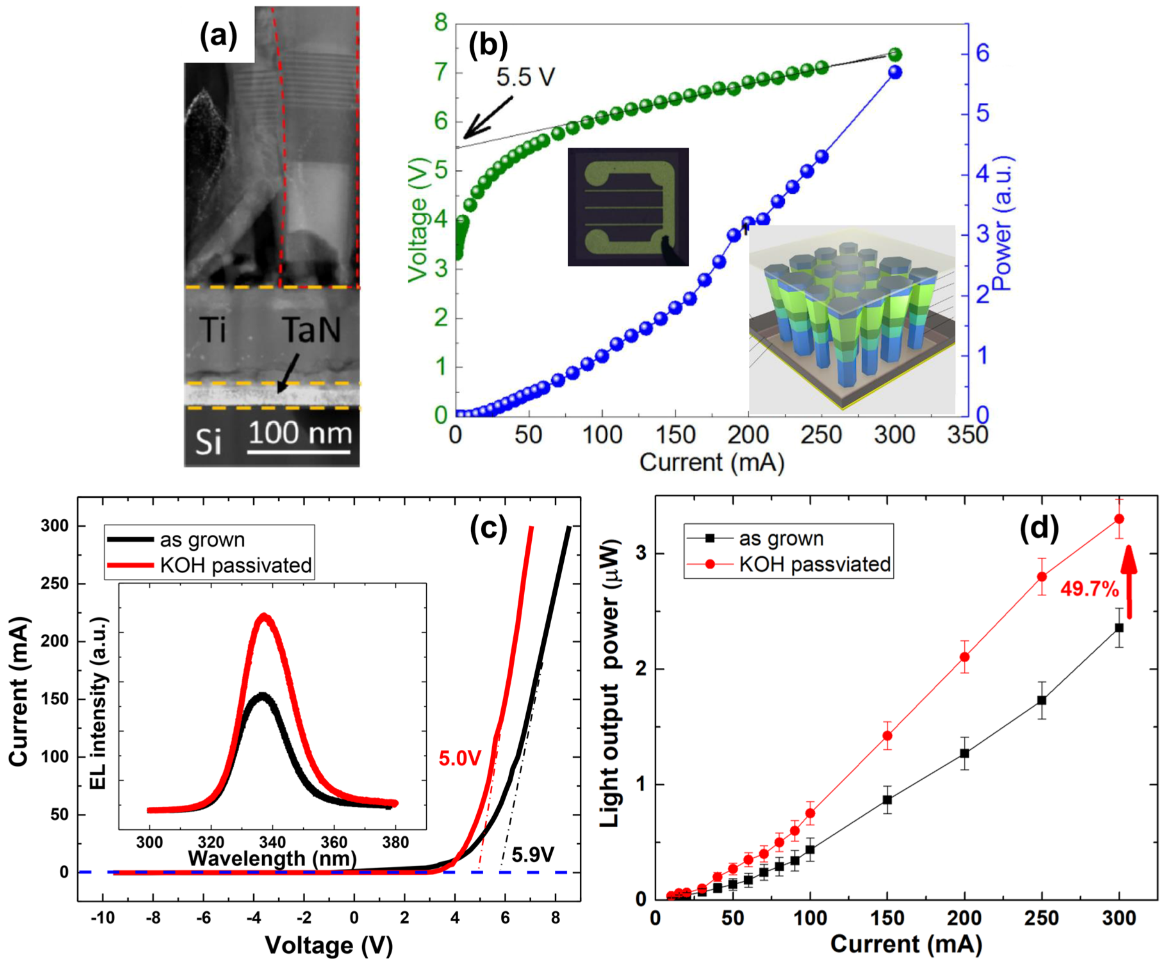

Figure 3. a) Cross-sectional HAADF-STEM image of AlGaN nanowires grown on Ti-coated Si substrate. b) Typical L–I–V characteristics of AlGaN nanowire UV LEDs, with the inset showing a photograph of probing a device and the schematic of fabricated nanowire LEDs. c) I–V characteristics before and after KOH passivation process. The inset shows the EL spectra. d) Output power before and after KOH passivation process. a) Reproduced with permission.[91] Copyright 2017, Optical Society of America. b) Reproduced with permission.[90] Copyright 2017, Optical Society of America. c,d) Reproduced with permission.[92] Copyright 2018, American Chemical Society.

2.4. III-Nitride Nanowire LEDs on Diamond

Beside metal substrates, diamond, due to its UV transparency and high thermal conductivity, has been exploited as the hetero-epitaxial wafer for III-nitride nanowires. Schuster et al. demonstrated the nucleation of self-assembled GaN nanowires on (111) single crystalline diamond without using any foreign catalyst and buffer layer.[96,97] A high-quality diamond/nanowire interface is measured, as shown in **Figure 5**(a). A strong and sharp excitonic emission measured in the photoluminescence (PL) experiment suggests excellent optical quality. They further fabricated nanodiodes utilizing n-GaN nanowires on p-diamond substrates. Figure 5(b) shows the I–V characteristics, exhibiting a rectification ratio of three orders of magnitude. The EL spectra are shown in Figure 5(c), consisting of two emission lines with a similar intensity: a broad green emission at 2.4 eV and a sharp UV emission at 3.4 eV due to the carrier recombination at both sides of the heterointerface.[97] Figure 5(d) shows a top view thermographic image (in arbitrary scale) of such a nanoLED device, suggesting an inhomogeneous Joule heating across the device. Further improving the nanowire size uniformity, together with a better top contact, would be the next step for diamond/nitride based light emitters.

2.5. III-Nitride Nanowire LEDs on 2D Materials

2D materials, for example, TMDCs,[98,99] graphene,[47,100,101] and boron nitride[13] owing to their strong in-plane bonding and weak out-of-plane interaction, have attracted significant attention as interfacial layer for the growth of III-nitrides, as they can serve as sacrificial layers for lifting-off III-nitride nanowires from the original substrates and thus enable the reuse of substrates, opening up new opportunities to fabricate low cost and large scale electronic and photonic devices.[47,99]

InGaN/GaN nanowire blue and yellow LEDs on large-area MoS_2-coated Mo substrates have been demonstrated.[99] The monolayer MoS_2 serves as both the buffer layer for nanowire growth and the sacrificial layer for epitaxial lift-off. As shown in **Figure 6**(a), the nanowire LEDs have a low turn-on voltage of

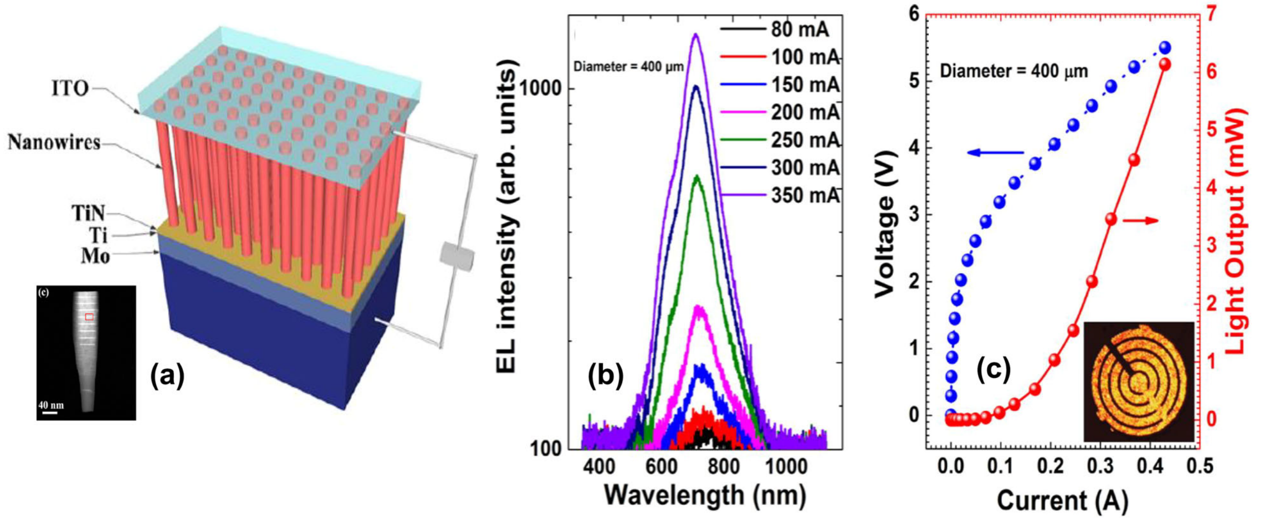

Figure 4. a) Schematic of InGaN/GaN nanowire LEDs on Ti-coated Mo substrate. The inset shows a HAADF-STEM image of an individual InGaN/GaN nanowire. b) EL spectra measured under injection currents from 80 to 350 mA. c) Measured L–I–V characteristics. The inset shows a photograph of an illuminated LED. Reproduced with permission.[45] Copyright 2016, American Chemical Society.

about 2 V, which is due to the existence of the metallic Mo_2N layer.[102] Also shown in Figure 6(a), a maximum output power of 1.5 mW is measured under an injection current of 1000 mA. Figure 6(b) shows the EL spectra under different injection currents, with the inset showing a photograph of an illuminated device emitting around 635 nm. In Section 3, we will further discuss the transfer of III-nitride nanowire LED structures with the removal of the 2D interfacial layer, which enables flexible LEDs.

3. Flexible III-Nitride Nanowire Photonic Devices Through Transfer

Various technologies have been investigated in the past for flexible integrated electronic and photonic devices. Organic LEDs (OLEDs),[103–105] due to their relatively mature manufacturing process, low cost, and bendability, are considered as the dominant flexible light emitting technologies for personal electronics, for example, cell phones. Moreover, hybrid perovskites have recently emerged as attractive materials for flexible light emitting devices, owing to their high color purity and tunable bandgap energies.[106–108] Colloidal quantum-dots (QDs) have also been proposed as another technology along this direction.[109–111] III-nitride nanowires, on the other hand, due to their extraordinary chemical and mechanical stability, flexibility in choosing underlying substrates, together with the ultra-wide bandgap tunability from deep UV to NIR, could be another candidate. Today, there are two approaches to realize III-nitride nanowire photonic devices on flexible substrates: direct growth and transfer.

3.1. Direct Growth

The first approach to fabricate nanowire flexible photonics is by growing those III-nitride nanowires directly on flexible

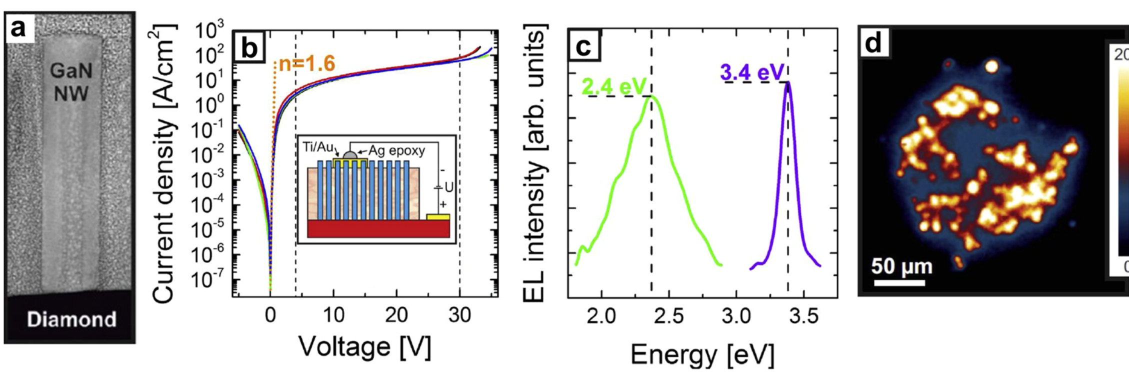

Figure 5. a) Cross-sectional HAADF-STEM image of a GaN nanowire on diamond substrate. b) I–V characteristics of n-GaN/p-diamond LEDs measured in different spots on the wafer. The inset illustrates the fabricated device. c) Room temperature EL spectra of a nanoLED device obtained at 30 V. d) A top view thermographic image of a device. a) Reproduced with permission.[44] Copyright 2016, Elsevier. b,c,d) Reproduced with permission.[97] Copyright 2015, AIP Publishing.

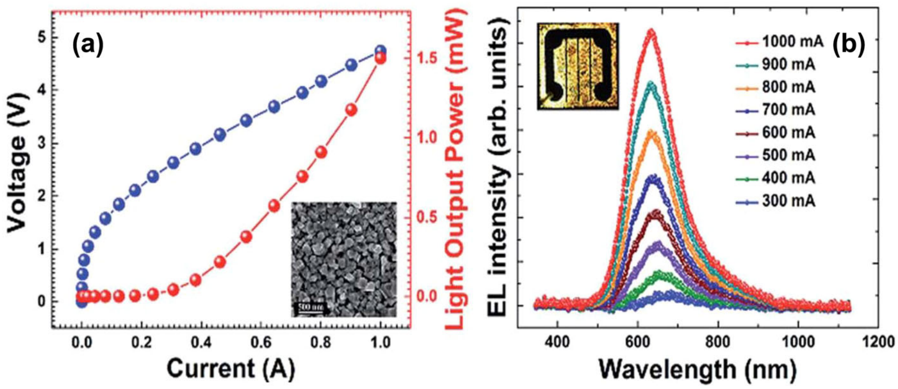

Figure 6. a) Typical L–I–V characteristics of InGaN/GaN nanowire LEDs on MoS_2-coated Mo substrates (device size: 500 μm × 500 μm). The inset shows an SEM image of InGaN/GaN nanowires. b) EL spectra of an LED at injection currents from 300 to 1000 mA. The inset shows a photograph of an illuminated LED. Reproduced with permission.[99] Copyright 2017, Royal Society of Chemistry.

substrates. Recently, direct growth of III-nitride nanowires on carbon paper[112] and functional AlGaN nanowire UV LEDs on Ta foils[58] have been demonstrated. May et al. reported a flexible UVLED by directly growing AlGaN nanowire on a flexible Ti foil, as shown in **Figure 7**(a,b). The nanowires are uniformly tilted with respect to the surface normal and the wires have similar heights and radii, and are evenly distributed throughout the region. The EL spectral of the flexible UVLED (Figure 7[c]) shows UV emission with a peak at 350 nm. The I–V curve (Figure 7[c] inset) shows good diode characteristics with a turn on voltage ≈5 V, comparable to the same heterostructure grown on n-Si. Although it is still at early stage and the results are preliminary, the realization of nanowire photonic devices directly on flexible metal foils provides an important step toward scalable roll-to-roll manufacturing of flexible photonics.

3.2. Transfer Via Epitaxial Lift-Off

Here, the majority research work hitherto focuses on the transfer of III-nitride nanowire structures to flexible substrates, which is summarized in **Table 1**. In this section, we discuss the transfer of III-nitride nanowire structures to flexible substrates, which enables flexible III-nitride nanowire photonic devices.

3.2.1. Single Nanowire Transfer

Individual nanowires, owing to their unique geometry, possess remarkable physical, chemical, and mechanical properties. Moreover, they are mechanically transferable, making them suitable for flexible photonic devices.[25] Various single nanowire transfer techniques have been developed. Shown in **Figure 8**(a), Lieber et al. transferred individual nanowires (red and purple lines representing two types of nanowires) to a plastic substrate.[25] Figure 8(b) shows an SEM image of two crossed-nanowire UV LEDs assembled from an n-type GaN nanowire and two p-type Si nanowires. Figure 8(c) is a photograph of the two illuminated LEDs. Such nanowire LEDs can maintain light emissive properties after multiple bending cycles.

Li et al. further demonstrated optically pumped single GaN nanowire lasers. The GaN nanowires are transferred from a c-

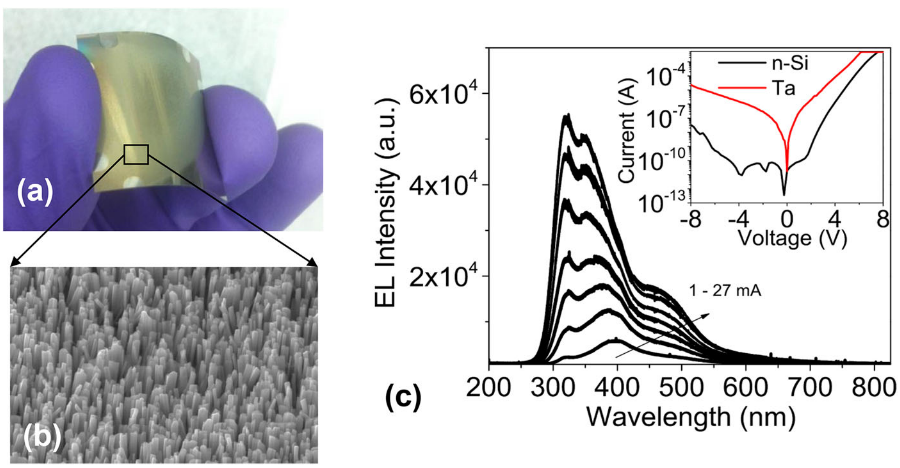

Figure 7. a,b) A photograph and SEM image of AlGaN nanowires on flexible Ti foil, respectively; (c) EL spectra of the fabricated nanowire LEDs; inset shows IV characteristics of LED on Ta (red) compared to a similar device on Si (black). Reproduced with permission.[58] Copyright 2016, AIP Publishing.

Table 1. Transfer of III-nitride nanowire structures to various substrates.

Type of nanowire	Orginal substrate	Destination substrate	Ref.
GaN nanowire	*c*-sapphire	Plastic	[25]
InGaN nanowire	*c*-sapphire	Copper tape and plastic scotch tape	[46]
GaN micro-rods	Graphene/SiO_2/Si	Polyimide substrate	[47]
InGaN nanowire	MoS_2/Mo	Polyethylene terephthalate (PET)	[99]
InGaN nanowire	*c*-sapphire	Metal foil	[113]
GaN/ZnO nanorod	Graphene/SiO_2/Si	Cu-coated (PET)	[114]
InGaN nanowire	Si	Bulk copper	[115]
GaN nanowire	*c*-sapphire	Si_3N_4	[116]
InGaN/GaN nanowires/disk	Amorphous SiO_2/Si	Polyimide sheet by Au welding	[117]

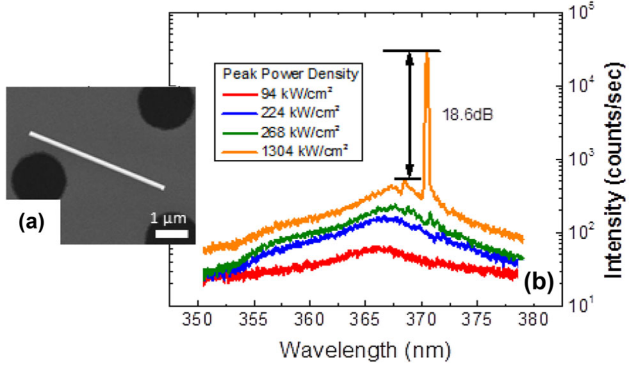

Figure 9. a) SEM image of a transferred GaN nanowire with a diameter of 135 nm and a length of 4.7 µm. b) Lasing spectra of a single GaN nanowire laser under different pump intensities. Reproduced with permission.[117] Copyright 2012, Optical Society of America.

plane sapphire substrate to a Si_3N_4 substrate after a top-down fabrication process.[116] An SEM of a transferred GaN nanowire is shown in **Figure 9**(a). Figure 9(b) shows the lasing spectra. It is seen that a single-mode lasing with a linewidth of 0.12 nm and a side mode suppression ratio >18 dB is measured.[116]

3.2.2. Nanowire Array Transfer Via Epitaxial Lift-Off

The complexity in positioning single nanowires and the integration with unconventional substrates may restrict their broad applications. In this regard, transferring large area bottom-up nanowires may appear more promising.

Chung et al. demonstrated flexible InGaN/GaN micro-rod LEDs by growing the micro-rods on graphene-coated Si substrate, followed by transferring them onto Ag-coated polymer substrate using lift-off.[47] The pre-transferred GaN micro-rod LED structures are vertically aligned on the graphene-coated Si substrate, as shown in **Figure 10**(a). Figure 10(b) illustrates the entire fabrication process of the flexible GaN micro-rod LEDs. Figure 10(c) shows the room temperature EL spectra of GaN micro-rod flexible LEDs at applied currents in the range 2.6–10 mA. The flexible micro-rod LEDs exhibit intense emission, as shown in the inset of Figure 10(c). Moreover, such flexible LEDs are found to exhibit stable emission even after numerous cycles of mechanical bending.

Dai et al. further demonstrated fully flexible blue LEDs based on core/shell InGaN/GaN nanowires at a large scale.[46] They transferred the InGaN nanowire arrays by embedding them in a flexible film, followed by peeling off those nanowires from the original sapphire substrate. Afterwards, the nanowires were transferred to a copper tape, forming flexible LEDs. The detailed fabrication process to produce flexible LEDs on the copper tape is illustrated in **Figure 11**(a–c). Photographs of such LEDs before and after current injection are shown in Figure 11(d,e),

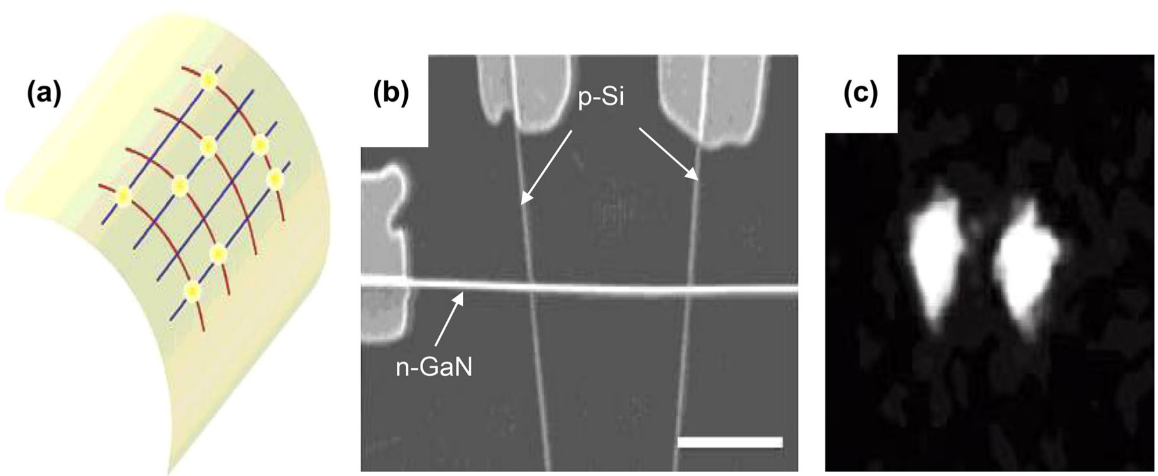

Figure 8. a) Schematic of LEDs on a plastic substrate. b) SEM image of two p-type Si nanowires crossing with an n-type GaN nanowire to form two LEDs. The scale bar is 1 µm. c) EL image of the localized light emission from the two Si-GaN junctions. Reproduced with permission.[25] Copyright 2003, American Chemical Society.

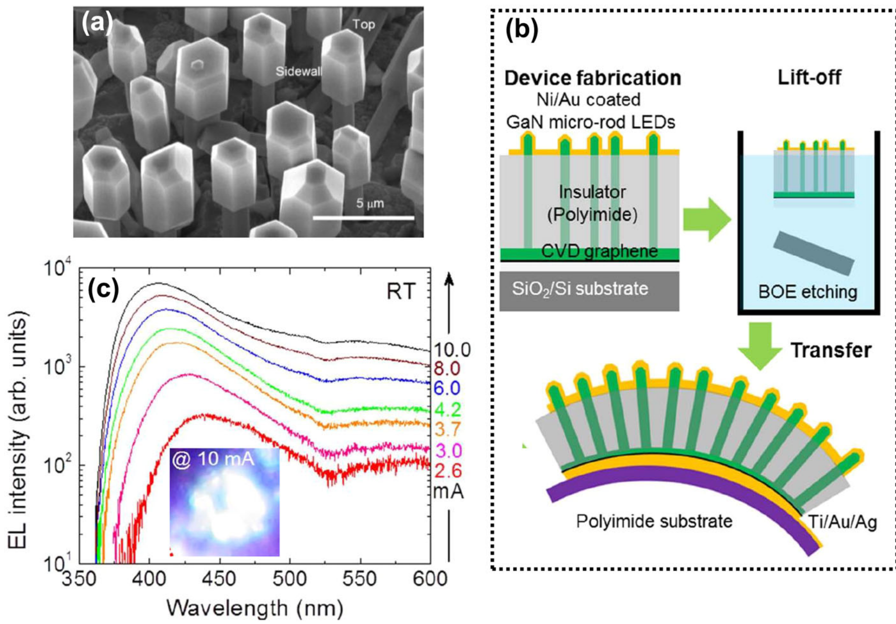

Figure 10. a) SEM image of GaN micro-rods on graphene-coated Si substrate. b) Schematic of the fabrication process for flexible GaN micro-rod LEDs. c) Room temperature EL spectra of a fabricated flexible GaN micro-rod LED. The inset shows an optical image of the light emission at an injection current of 10 mA ($50 \times 50\,\mu m^2$). Reproduced with permission.[47] Copyright 2014, AIP Publishing.

respectively. The turn-on voltage of such LEDs is around 3.5 V, with a relatively broad EL emission, as illustrated in Figure 11(f).

Moreover, the PDMS layer can be doped with YAG:Ce phosphors (as schematically shown in **Figure 12**[a]) to down-convert blue light and produce white light. The EL spectra and CIE 1931 chromaticity diagram are shown in Figure 12(b,c), respectively.[113] The inset of Figure 12(b) shows a flexible white color emitting nanowire LED chip. Moreover, by stacking a green LED membrane on top of a blue LED membrane or vice versa, with independent power supply for each membrane, a two-layer bicolor nanowire based flexible LEDs are further

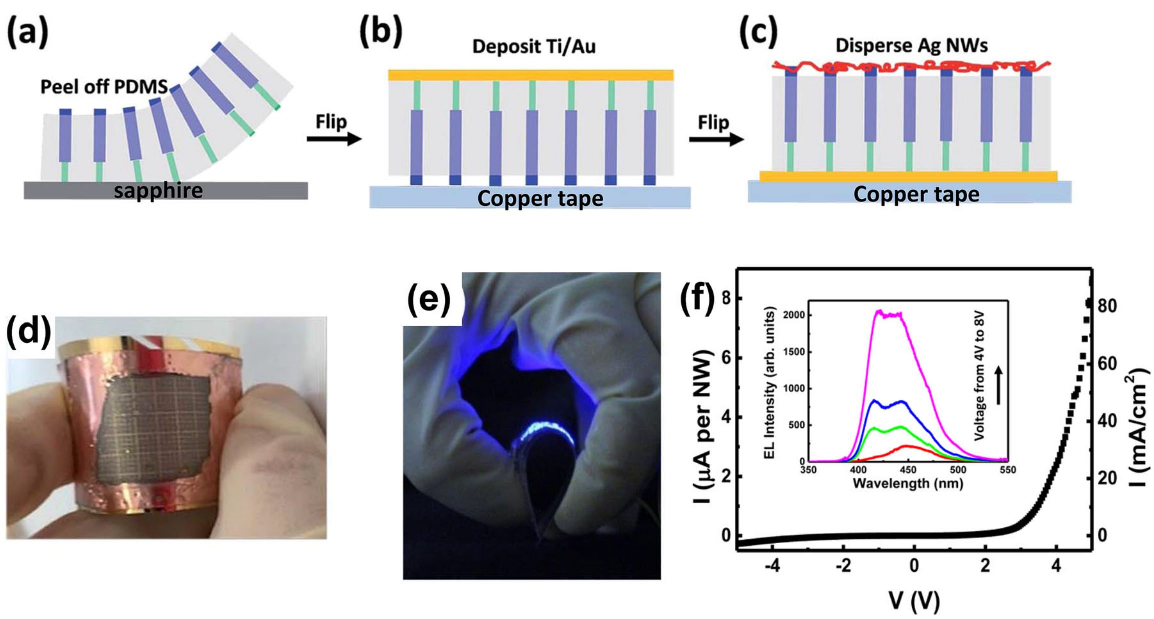

Figure 11. a–c) Schematic of the fabrication process for semitransparent LEDs with Ti/Au and Ag nanowires as the back and top contacts, respectively. d) A photograph of such semitransparent LEDs on a copper tape. e) A photograph of an LED chip emitting blue light at a curvature radius of 3.5 mm (chip size: $15 \times 6.5\,mm^2$). f) I–V characteristics of the flexible LEDs. The inset presents the room temperature EL spectra at various applied biases from 4 to 8 V. Reproduced with permission.[46] Copyright 2015, American Chemical Society.

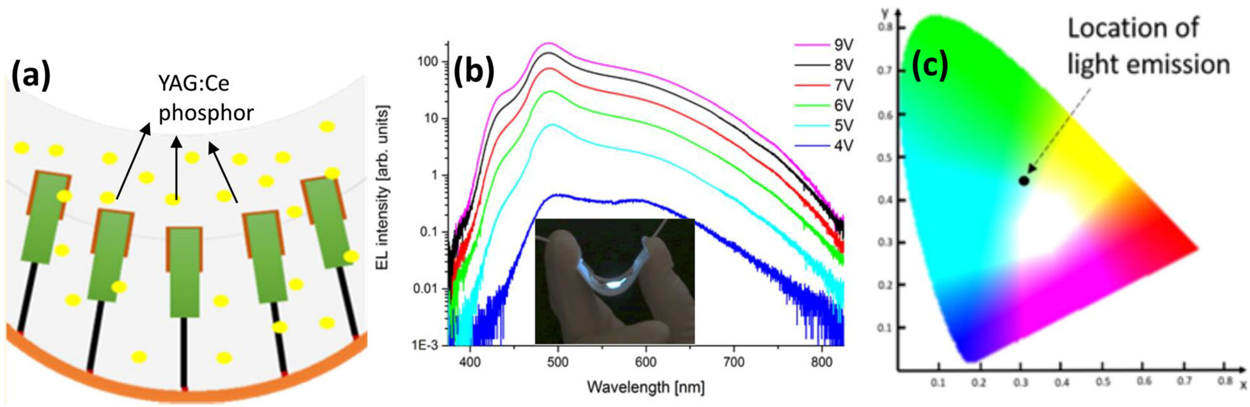

Figure 12. a) Schematic of the InGaN/GaN nanowire LED structures embedded in the polymer doped with YAG:Ce yellow phosphor. b) EL spectra of the flexible white color emitting LEDs under biases from 4 to 9 V. The inset shows a photograph of the operating flexible white color emitting LEDs under a bending radius of -5 mm (chip size: $5 \times 6\,mm^2$). c) CIE 1931 chromaticity diagram of such flexible white color emitting LEDs under an injection current density of $3.9\,A\,cm^{-2}$ (chromaticity coordinates $x = 0.3011$, $y = 0.4688$; CCT = 6306 K; CRI = 54). Reproduced with permission.[113] Copyright 2016, American Chemical Society.

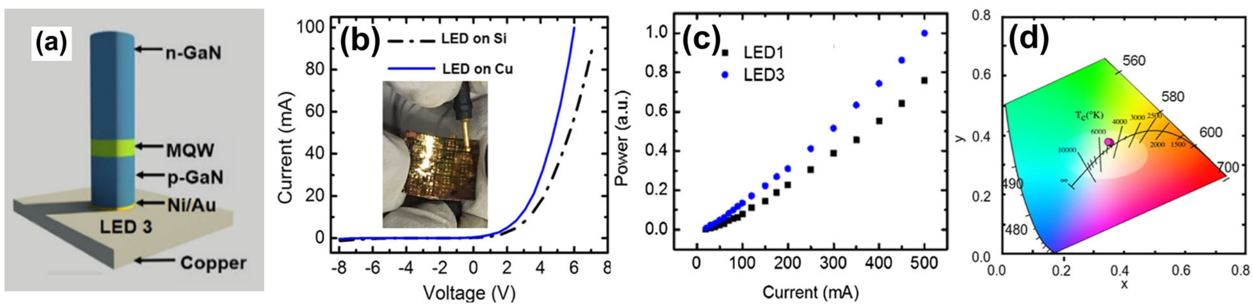

Figure 13. a) Schematic of the transferred InGaN/GaN nanowire LED structure on copper substrate. b,c) I–V characteristics and output power of the conventional nanowire LEDs on Si substrate (LED 1) and nanowire LEDs on copper (LED 3), respectively (chip size of $1 \times 1\,mm^2$). The inset of (b) shows a photograph of the LED chip on copper substrate. d) CIE diagram of LEDs on copper substrate. Reproduced with permission.[116] Copyright 2017, American Chemical Society.

demonstrated.[46] This lift-off and transfer procedure enables the assembly of free-standing layers of nanowire LEDs emitting at different wavelengths, and opens a new path to develop nanowire based high brightness flexible white or multi-color LEDs.

Recently, Philip et al. reported the transfer of InGaN/AlGaN nanowire LED structures grown on Si to a copper substrate.[115] **Figure 13**(a) shows the schematic of the transferred LED structure. Since copper substrate has better heat dissipation and electrical conductivity compared to Si, the LEDs on the copper substrate exhibit improved I–V characteristics with lower leakage current and higher output power comparing to the LEDs on Si, as shown in Figure 13(b,c), respectively. The LEDs on copper show a CRI of around 95 (Figure 13[d]). Similar device performance improvement has also been observed after transferring InGaN/GaN nanowire heterostructures grown on a 200 nm amorphous SiO_2 layer on Si substrate to a flexible polyimide sheet by Au-welding and epitaxial lift-off processes.[117] The transferred nanowire LEDs, emitting at 600 nm, showed a smaller turn-on voltage in contrast to those of as-grown nanowire LEDs due to the absence of an intermediate Si_xN_y layer.[117]

4. Conclusions and Prospects

In this paper, we have reviewed recent progresses of III-nitride nanowire LEDs and lasers on various foreign substrates. Some state of the art performance devices have been demonstrated. For example, AlN nanowire LEDs on Si possess the best I–V characteristics comparing to any other AlN structures. Also, using AlGaN nanowire structures, the electrically injected lasing in the deep UV spectral range is measured, being the only semiconductor structure that is able to produce lasing in the deep UV spectral range through direct electrical injection. The flexibility in choosing substrates also enables III-nitride nanowire based flexible photonic devices. For example, by transferring III-nitride nanowire LED structures to various flexible substrates, flexible III-nitride nanowire LEDs emitting in the visible spectral range have been demonstrated, making III-nitride nanowires to be a promising candidate for flexible integrated photonics.

There are, however, a number of challenges to overcome before delivering practical III-nitride nanowire based flexible photonic devices. First of all, the growth process of III-nitride nanowires are highly dynamic, making the growth optimization is not as straightforward as that of III-nitride epilayers. Finding a solution to precisely monitor the growth of III-nitride nanowires, and further correlating with their electrical and optical properties, are critically important to provide high performance flexible III-nitride nanowire photonic devices. Secondly, optimization of the device fabrication process, including the packaging technologies, is more complicated compared to that of conventional planar devices; and some challenges are quite unique to nanowire devices. For example, due to the presence of gaps among nanowire arrays, making metal contacts to nanowire device structures, which can spread current uniformly and yet fully transparent, has remained challenging. Thirdly, hitherto MBE has been the dominant technique to produce high quality III-nitride nanowire heterostructures; and III-nitride nanowires, in particular AlGaN nanowires, grown with CVD techniques generally show inferior qualities due to the unwanted contamination (e.g., due to the use of low purity source materials), lack of accurate control on the temperature of each source, and in some cases, the use of foreign catalysts that degrade the electrical and optical qualities. In this regard, it is imperative to find a low-cost approach to produce large-scale materials with reasonably good quality, which can be transferred to devices with similar performance to that of conventional epilayers, as a viable path to mass production of flexible III-nitride nanowire photonic devices. Addressing these issues properly and in a timely manner, together with the development of other photonic components such as lasers, photodetectors, could enable III-nitride nanowires to be a competing technology for flexible integrated photonics.

Acknowledgement

We acknowledge the supports of KAUST Baseline BAS/1/1664-01-01, KAUST Competitive Research Grant URF/1/3437-01-01, and GCC Research Council REP/1/3189-01-01. The authors are also thankful to Prof. Songrui Zhao from McGill University for sharing ideas contributed to this article. This article was amended on December17, 2018 to correct the authorship and the acknowledgement section.

Conflict of Interest

The author declares no conflict of interest.

Keywords

III-nitride nanowires, flexible photonics, foreign substrate, lasers, light emitting diodes

Received: June 5, 2018
Revised: August 16, 2018
Published online: October 24, 2018

[1] T. D. Moustakas, R. Paiella, *Rep. Prog. Phys.* **2017**, *80*, 106501.
[2] S. Zhao, H. P. T. Nguyen, M. G. Kibria, Z. Mi, *Prog. Quantum Electron.* **2015**, *44*, 14.
[3] D. B. Li, K. Jiang, X. J. Sun, C. L. Guo, *Adv. Optic. Photon.* **2018**, *10*, 43.
[4] G. Li, W. Wang, W. Yang, Y. Lin, H. Wang, Z. Lin, S. Zhou, *Rep. Prog. Phys.* **2016**, *79*, 056501.
[5] W. Guo, H. Sun, B. Torre, J. Li, M. Sheikhi, J. Jiang, H. Li, S. Guo, K. Li, R. Lin, A. Giugni, E. D. Fabrizio, X. Li, J. Ye, *Adv. Funct. Mater.* **2018**, *28*, 1802395.
[6] Z. Zhang, Y. Zhang, W. Bi, H. V. Demir, X. W. Sun, *Phys. Status Solidi A* **2016**, *213*, 3078.
[7] L. Li, Y. Zhang, S. Xu, W. Bi, Z. Zhang, H. Kuo, *Materials* **2017**, *10*, 1221.
[8] H. Sun, J. Yin, E. F. Pecora, L. D. Negro, R. Paiella, T. D. Moustakas, *IEEE Photon. J.* **2017**, *9*, 2201109.
[9] E. F. Pecora, H. Sun, L. Dal Negro, T. D. Moustakas, *Opt. Mater. Exp.* **2015**, *5*, 809.
[10] H. Sun, E. F. Pecora, J. Woodward, D. J. Smith, L. Dal Negro, T. D. Moustakas, *Phys. Status Solidi A* **2016**, *213*, 1165.
[11] H. M. Kim, J. E. Oh, T. W. Kang, *Mater. Lett.* **2001**, *47*, 276.
[12] N. R. Glavin, K. D. Chabak, E. R. Heller, E. A. Moore, T. A. Prusnick, B. Maruyama, D. E. Walker, D. L. Dorsey, Q. Paduano, M. Snure, *Adv. Mater.* **2017**, *29*, 1701838.
[13] Y. Kobayashi, K. Kumakura, T. Akasaka, T. Makimoto, *Nature* **2012**, *484*, 223.
[14] W. S. Wong, T. Sands, N. W. Cheung, M. Kneissl, D. P. Bour, P. Mei, L. T. Romano, N. M. Johnson, *Appl. Phys. Lett.* **1999**, *75*, 1360.
[15] L. Wang, J. Ma, Z. Liu, X. Yi, H. Zhu, G. Wang, *ACS Photon.* **2014**, *1*, 421.
[16] P. Tian, J. J. D. McKendry, E. Gu, Z. Chen, Y. Sun, G. Zhang, M. D. Dawson, R. Liu, *Opt. Express* **2016**, *24*, 699.
[17] J. Chun, Y. Hwang, Y. S. Choi, T. Jeong, J. H. Baek, H. C. Ko, S. J. Park, *IEEE Photon. Technol. Lett.* **2012**, *24*, 2115.
[18] H. K. Cho, O. Krüger, A. Külberg, J. Rass, U. Zeimer, T. Kolbe, A. Knauer, S. Einfeldt, M. Weyers, M. Kneissl, *Semicond. Sci. Technol.* **2017**, *32*, 12LT01.
[19] D. Hwang, B. P. Yonkee, B. S. Addin, R. M. Farrell, S. Nakamura, J. S. Speck, S. DenBaars, *Opt. Express* **2016**, *24*, 22875.
[20] C. O. Holder, J. T. Leonard, R. M. Farrell, D. A. Cohen, B. Yonkee, J. S. Speck, S. P. DenBaars, S. Nakamura, D. F. Feezell, *Appl. Phys. Lett.* **2014**, *105*, 031111.
[21] B. P. Yonkee, B. SaifAddin, J. T. Leonard, S. P. DenBaars, S. Nakamura, *Appl. Phys. Express* **2016**, *9*, 056502.
[22] C. K. Jeong, K.-I. Park, J. H. Son, G.-T. Hwang, S. H. Lee, D. Y. Park, H. E. Lee, H. K. Lee, M. Byun, K. J. Lee, *Energy Environ. Sci.* **2014**, *7*, 4035.
[23] S.-I. Park, A.-P. Le, J. Wu, Y. Huang, X. Li, J. A. Rogers, *Adv. Mater.* **2010**, *22*, 3062.
[24] K. Chung, C.-H. Lee, G.-C. Yi, *Science* **2010**, *330*, 655.
[25] M. C. Mcalpine, R. S. Friedman, S. Jin, K.-H. Lin, W. U. Wang, C. M. Lieber, *Nano Lett.* **2003**, *3*, 1531.
[26] C. Ning, L. Dou, P. Yang, *Nat. Rev. Mater.* **2017**, *2*, 17070.
[27] F. Glas, *Phys. Rev. B.* **2006**, *74*, 121302.
[28] E. Galopin, L. Largeau, G. Patriarche, L. Travers, F. Glas, J. C. Harmand, *Nanotechnology* **2011**, *22*, 245606.
[29] N. Tran, B. Le, S. Zhao, Z. Mi, *Appl. Phys. Lett.* **2017**, *110*, 032102.
[30] S. Zhao, B. Le, D. Liu, X. D. Liu, M. Kibria, T. Szkopek, H. Guo, Z. Mi, *Nano Lett.* **2013**, *13*, 5509.
[31] D. E. Perea, E. R. Hemesath, E. J. Schwalbach, J. L. Lensch-Falk, P. W. Voorhees, L. J. Lauhon, *Nat. Nanotechnol.* **2009**, *4*, 315.
[32] J. C. Ho, R. Yerushalmi, Z. A. Jacobson, Z. Fan, R. L. Alley, A. Javey, *Nat. Mater.* **2008**, *7*, 62.
[33] P. Xie, Y. Hu, Y. Fang, J. Huang, C. M. Lieber, *Proc. Natl. Acad. Sci.* **2009**, *106*, 5254.
[34] E. Koren, N. Berkovitch, Y. Rosenwaks, *Nano Lett.* **2010**, *10*, 1163.
[35] J. E. Allen, D. E. Perea, E. R. Hemesath, L. J. Lauhon, *Adv. Mater.* **2009**, *21*, 3067.

[36] S. Zhao, A. T. Connie, M. H. Dastjerdi, X. H. Kong, Q. Wang, M. Djavid, S. Sadaf, X. D. Liu, I. Shih, H. Guo, Z. Mi, *Sci. Rep*. **2015**, *5*, 8332.
[37] S. Zhao, X. Liu, Y. Wu, Z. Mi, *Appl. Phys. Lett*. **2016**, *109*, 191106.
[38] S. Zhao, S. Y. Woo, M. Bugnet, X. Liu, J. Kang, G. A. Botton, Z. Mi, *Nano Lett*. **2015**, *15*, 7801.
[39] S. Zhao, X. Liu, S. Y. Woo, J. Kang, G. A. Botton, Z. Mi, *Appl. Phys. Lett*. **2015**, *107*, 043101.
[40] A. Hazari, F. C. Hsiao, L. Yan, J. Heo, J. M. Millunchick, J. M. Dallesasse, P. Bhattacharya, *IEEE J. Quantum Electron*. **2017**, *53*, 1.
[41] A. T. M. G. Sarwar, S. D. Carnevale, F. Yang, T. F. Kent, J. J. Jamison, D. W. McComb, R. C. Myers, *Small* **2015**, *11*, 5402.
[42] V. Kumaresan, L. Largeau, A. Madouri, F. Glas, H. Zhang, F. Oehler, A. Cavanna, A. Babichev, L. Travers, N. Gogneau, M. Tchernycheva, J.-C. Harmand, *Nano Lett*. **2016**, *16*, 4895.
[43] M. Heilmann, A. M. Munshi, G. Sarau, M. Göbelt, C. Tessarek, V. T. Fauske, A. T. J. van Helvoort, J. Yang, M. Latzel, B. Hoffmann, G. Conibeer, H. Weman, S. Christiansen, *Nano Lett*. **2016**, *16*, 3524.
[44] M. Hetzl, F. Schuster, A. Winnerl, S. Winnerl, M. Stutzmann, *Mater. Sci. Semicond. Process*. **2016**, *48*, 65.
[45] C. Zhao, T. K. Ng, R. T. ElAfandy, A. Prabaswara, G. B. Consiglio, I. A. Ajia, I. S. Roqan, B. Janjua, C. Shen, J. Eid, A. Y. Alyamani, M. M. El-Desouki, B. S. Ooi, *Nano Lett*. **2016**, *16*, 4616.
[46] X. Dai, A. Messanvi, H. Zhang, C. Durand, J. Eymery, C. Bougerol, F. H. Julien, M. Tchernycheva, *Nano Lett*. **2015**, *15*, 6958.
[47] K. Chung, H. Beak, Y. Tchoe, H. Oh, H. Yoo, M. Kim, G.-C. Yi, *APL Mater*. **2014**, *2*, 092512.
[48] S. Zhao, Z. Mi, *Semiconduct. Semimet*. **2017**, *96*, 267.
[49] S. Zhao, *Semiconduct. Semimet*. **2017**, *96*, 167.
[50] H. Li, G. Zhao, H. Wei, L. Wang, Z. Chen, S. Yang, *Nanoscale Res. Lett*. **2016**, *11*, 270.
[51] M. Sobanska, S. Fernández-Garrido, Z. R. Zytkiewicz, G. Tchutchulashvili, S. Gieraltowska, O. Brandt, L. Geelhaar, *Nanotechnology* **2016**, *27*, 325601.
[52] A. Liudi Mulyo, Y. Konno, J. S. Nilsen, A. T. J. van Helvoort, B. Fimland, H. Weman, K. J. Kishino, *J. Cryst. Growth* **2017**, *480*, 67.
[53] S.-Y. Bae, J.-W. Min, H.-Y. Hwang, K. Lekhal, H.-J. Lee, Y.-D. Jho, D. S. Lee, Y. T. Lee, N. Ikarashi, Y. Honda, H. Amano, *Sci. Rep*. **2017**, *7*, 45345.
[54] Y. Zhang, J. Liu, R. He, Q. Zhang, X. Zhang, J. Zhu, *Chem. Mater*. **2001**, *13*, 3899.
[55] J. Johnson, H. Choi, K. P. Knutsen, R. D. Schaller, P. Yang, R. J. Saykally, *Nat. Mater*. **2002**, *1*, 106.
[56] N. Alfaraj, M. M. Muhammed, K.-H. Li, B. Janjua, R. A. Aljefri, H. Sun, T. K. Ng, B. S. Ooi, I. S. Roqan, X. Li, *AIP Adv*. **2017**, *7*, 125113.
[57] B. Janjua, T. K. Ng, C. Zhao, H. M. Oubei, C. Shen, A. Prabaswara, M. S. Alias, A. A. Alhamoud, A. A. Alatawi, A. M. Albadri, A. Y. Alyamani, M. M. El-Desouki, B. S. Ooi, *Opt. Express* **2016**, *24*, 19228.
[58] B. J. May, A. T. M. G. Sarwar, R. C. Myers, *Appl. Phys. Lett*. **2016**, *108*, 141103.
[59] H. Sun, D. Priante, J.-W. Min, R. C. Subedi, M. K. Shakfa, Z. Ren, K.-H. Li, R. Lin, C. Zhao, T. Ng, J.-H. Ryou, X. Zhang, B. S. Ooi, X. Li, *ACS Photon*. **2018**, *5*, 3305.
[60] X. Duan, C. M. J. Lieber, *Am. Chem. Soc*. **2000**, *12*, 738.
[61] E. Calleja, M. A. Sánchez-García, F. J. Sánchez, F. Calle, F. B. Naranjo, E. Munoz, S. I. Molina, A. M. Sanchez, F. J. Pacheco, R. J. Garcıa, *J. Cryst. Growth* **1999**, *201/202*, 296.
[62] M. Yoshizawa, A. Kikuchi, N. Fujita, K. Kushi, H. Sasamoto, K. J. Kishino, *J. Cryst. Growth* **1998**, *189/190*, 138.
[63] T. Tang, S. Han, W. Jin, X. L. Liu, C. Li, D. H. Zhang, C. W. Zhou, B. Chen, J. Han, M. J. Meyyappan, *Mater. Res*. **2004**, *19*, 423.
[64] C. C. Chen, C. C. Yeh, *Adv. Mater*. **2000**, *12*, 738.
[65] T. Kuykendall, P. Pauzauskie, S. Lee, Y. Zhang, J. Goldberger, P. Yang, *Nano Lett*. **2003**, *3*, 1063.
[66] K. Kishino, K. Nagashima, K. Yamano, *Appl. Phys. Express* **2013**, *6*, 012101.
[67] K. Kishino, A. Yanagihara, K. Ikeda, K. Yamano, *Electron. Lett*. **2015**, *51*, 852.
[68] K. Kishino, H. Sekiguchi, A. J. Kikuchi, *J. Cryst. Growth* **2009**, *311*, 2063.
[69] R. S. Wagner, W. C. Ellis, *Appl. Phys. Lett*. **1964**, *4*, 89.
[70] C. B. Maliakkal, N. Hatui, R. D. Bapat, B. A. Chalke, A. A. Rahman, A. Bhattacharya, *Nano Lett*. **2016**, *16*, 7632.
[71] C. Chèze, L. Geelhaar, O. Brandt, W. M. Weber, H. Riechert, S. Münch, R. Rothemund, S. Reitzenstein, A. Forchel, T. Kehagias, P. Komninou, *Nano Res*. **2010**, *3*, 528.
[72] S. D. Hersee, X. Sun, X. Wang, *Nano Lett*. **2006**, *6*, 1808.
[73] T. Auzelle, B. Daudin, *Semiconduct. Semimet*. **2017**, *96*, 203.
[74] R. Wang, H. P. Nguyen, A. T. Connie, J. Lee, I. Shih, Z. Mi, *Opt. Express* **2014**, *22*, A1768.
[75] H. P. T. Nguyen, K. Cui, S. Zhang, S. Fathololoumi, Z. Mi, *Nanotechnology* **2011**, *22*, 445202.
[76] T. Frost, S. Jahangir, E. Stark, S. Deshpande, A. Hazari, C. Zhao, B. S. Ooi, P. Bhattacharya, *Nano Lett*. **2014**, *14*, 4535.
[77] S. Jahangir, T. Frost, A. Hazari, L. Yan, E. Stark, T. LaMountain, J. M. Millunchick, B. S. Ooi, P. Bhattacharya, *Appl. Phys. Lett*. **2015**, *106*, 071108.
[78] R. Wang, Y. H. Ra, Y. Wu, S. Zhao, H. P. Nguyen, I. Shih, Z. Mi, *Proc. SPIE* **2016**, *9748*, 97481S-1.
[79] R. Wang, X. Liu, I. Shih, Z. Mi, *Appl. Phys. Lett*. **2015**, *106*, 261104.
[80] S. M. Sadaf, Y. H. Ra, H. P. T. Nguyen, M. Djavid, Z. Mi, *Nano Lett*. **2015**, *15*, 6696.
[81] S. Zhao, M. Djavid, Z. Mi, *Nano Lett*. **2015**, *15*, 7006.
[82] Y. Taniyasu, M. Kasu, T. Makimoto, *Nature* **2006**, *441*, 325.
[83] D. A. Laleyan, S. Zhao, S. Y. M. Woo, H. N. Tran, H. B. Le, T. Szkopek, H. Guo, G. A. Botton, Z. Mi, *Nano Lett*. **2017**, *17*, 3738.
[84] K. H. Li, X. Liu, Q. Wang, S. Zhao, Z. Mi, *Nat. Nanotechnol*. **2015**, *10*, 140.
[85] B. Janjua, H. Sun, C. Zhao, D. H. Anjum, F. Wu, A. A. Alhamoud, X. Li, A. M. Albadri, A. Y. Alyamani, M. M. El-Desouki, T. K. Ng, B. S. Ooi, *Nanoscale* **2017**, *9*, 7805.
[86] M. Wölz, C. Hauswald, T. Flissikowski, T. Gotschke, S. Fernández-Garrido, O. Brandt, H. T. Grahn, L. Geelhaar, H. Riechert, *Nano Lett*. **2015**, *15*, 3743.
[87] G. Calabrese, P. Corfdir, G. Gao, C. Pf̈uller, A. Trampert, O. Brandt, L. Geelhaar, S. Fernández-Garrido, *Appl. Phys. Lett*. **2016**, *108*, 202101.
[88] D. van Treeck, G. Calabrese, J. J. W. Goertz, V. M. Kaganer, O. B. Sergio Fernández-Garrido, L. Geelhaar, *Nano Res*. **2018**, *11*, 565.
[89] B. Janjua, T. K. Ng, C. Zhao, A. Prabaswara, G. B. Consiglio, D. Priante, C. Shen, R. T. Elafandy, D. H. Anjum, A. A. Alhamoud, A. A. Alatawi, Y. Yang, A. Y. Alyamani, M. M. El-Desouki, B. S. Ooi, *ACS Photon*. **2016**, *3*, 2089.
[90] B. Janjua, H. Sun, C. Zhao, D. H. Anjum, D. Priante, A. A. Alhamoud, F. Wu, X. Li, A. M. Albadri, A. Y. Alyamani, M. M. El-Desouki, T. K. Ng, B. S. Ooi, *Opt. Express* **2017**, *25*, 1381.
[91] D. Priante, B. Janjua, A. Prabaswara, R. C. Subedi, R. T. Elafandy, S. D. Lopatin, H. Anjum, C. Zhao, T. K. Ng, B. S. Ooi, *Opt. Mater. Express* **2017**, *7*, 4214.
[92] H. Sun, M. K. Shakfa, M. Mufasila, B. Janjua, K.-H. Li, R Lin, I. Roqan, B. S. Ooi, X. Li, *ACS Photon*. **2018**, *5*, 964.
[93] C. Zhao, T. K. Ng, A. Prabaswara, M. Conroy, S. Jahangir, T. Frost, J. O'Connell, J. D. Holmes, P. J. Parbrook, P. Bhattacharya, B. S. Ooi, *Nanoscale* **2015**, *7*, 16658.

[94] K. Ohkawa, T. Watanabe, M. Sakamoto, A. Hirako, M. J. Deura, *J. Cryst. Growth* **2012**, *343*, 13.
[95] C. Zhao, T. K. Ng, N. Wei, A. Prabaswara, M. S. Alias, B. Janjua, C. Shen, B. S. Ooi, *Nano Lett*. **2016**, *16*, 1056.
[96] F. Schuster, F. Furtmayr, R. Zamani, C. Magén, J. R. Morante, J. Arbiol, J. A. Garrido, M. Stutzmann, *Nano Lett*. **2012**, *12*, 2199.
[97] F. Schuster, M. Hetzl, S. Weiszer, M. Wolfer, H. Kato, C. E. Nebel, J. A. Garrido, M. Stutzmann, *J. Appl. Phys*. **2015**, *118*, 154303.
[98] Z. Zhu, J. Yuan, H. Zhou, J. Hu, J. Zhang, C. Wei, F. Yu, S. Chen, Y. Lan, Y. Yang, Y. Wang, C. Niu, Z. Ren, J. Lou, Z. Wang, J. Bao, *ACS Photon*. **2016**, *3*, 869.
[99] C. Zhao, T. K. Ng, C.-C. Tseng, J. Li, Y. Shi, N. Wei, D. Zhang, G. B. Consiglio, A. Prabaswara, A. A. Alhamoud, A. M. Albadri, A. Y. Alyamani, X. X. Zhang, L.-J. Li, B. S. Ooi, *RSC Adv.* **2017**, *7*, 26665.
[100] Y. Kim, S. S. Cruz, K. Lee, B. O. Alawode, C. Choi, Y. Song, J. M. Johnson, C. Heidelberger, W. Kong, S. Choi, K. Qiao, I. Almansouri, E. A. Fitzgerald, J. Kong, A. M. Kolpak, J. Hwang, J. Kim, *Nature* **2017**, *544*, 340.
[101] Z. Zeng, Z. Yin, X. Huang, H. Li, Q. He, G. Lu, F. Boey, H. Zhang, *Angew. Chem. Int. Ed*. **2011**, *50*, 11093.
[102] K. Inumaru, K. Baba, S. Yamanaka, *Chem. Mater.* **2005**, *17*, 5935.
[103] S. Scholz, D. Kondakov, B. Lüssem, K. Leo, *Chem. Rev.* **2015**, *115*, 8449.
[104] K. T. Ly, R. W. Chen-Cheng, H. W. Lin, Y. J. Shiau, S. H. Liu, P. T. Chou, C. S. Tsao, Y. C. Huang, Y. Chi, *Nat. Photon*. **2017**, *11*, 63.
[105] Q. Zhang, B. Li, S. Huang, H. Nomura, H. Tanaka, C. Adachi, *Nat. Photon*. **2014**, *8*, 326.
[106] X. Zhang, B. Xu, J. Zhang, Y. Gao, Y. Zheng, K. Wang, X. W. Sun, *Adv. Funct. Mater.* **2016**, *26*, 4595.
[107] X. Li, F. Cao, D. Yu, J. Chen, Z. Sun, Y. Shen, Y. Zhu, L. Wang, Y. Wei, Y. Wu, H. Zeng, *Small* **2017**, *13*, 1603996.
[108] B. R. Sutherland, E. H. Sargent, *Nat. Photon*. **2016**, *10*, 295.
[109] Y. Shirasaki, G. J. Supran, M. G. Bawendi, V. Bulovic, *Nat. Photon*. **2013**, *7*, 13.
[110] M. Liu, O. Voznyy, R. Sabatini, F. P. G. de Arquer, R. Munir, A. H. Balawi, X. Lan, F. Fan, G. Walters, A. R. Kirmani, S. Hoogland, F. Laquai, A. Amassian, E. H. Sargent, *Nat. Mater.* **2017**, *16*, 258.
[111] H. Zhang, S. Chen, X. W. Sun, *ACS Nano* **2018**, *12*, 697.
[112] M. A. Mastro, T. J. Anderson, M. J. Tadjer, F. J. Kub, J. K. Hite, J. Kim, C. R. Eddy, Jr., *Phys. Status Solidi C* **2018**, *11*, 442.
[113] N. Guan, X. Dai, A. Messanvi, H. Zhang, J. Yan, E. Gautier, C. Bougerol, F. H. Julien, C. Durand, J. Eymery, M. Tchernycheva, *ACS Photon*. **2016**, *3*, 597.
[114] C.-H. Lee, Y.-J. Kim, Y. J. Hong, S.-R. Jeon, S. Bae, B. H. Hong, G.-C. Yi, *Adv. Mater.* **2011**, *23*, 4614.
[115] M. R. Philip, D. D. Choudhary, M. Djavid, M. N. Bhuyian, T. H. Q. Bui, D. Misra, A. Khreishah, J. Piao, H. D. Nguyen, K. Q. Le, H. P. T. Nguyen, *ACS Omega* **2017**, *2*, 5708.
[116] Q. Li, J. B. Wright, W. W. Chow, T. S. Luk, I. Brener, L. F. Lester, G. T. Wang, *Opt. Express* **2012**, *20*, 17873.
[117] Y. Park, S. Jahangir, Y. Park, P. Bhattacharya, J. Heo, *Opt. Express* **2015**, *23*, A650.